Article

Theoretical Analysis of the Smallest Carbon Cluster Containing a Planar Tetracoordinate Carbon

Gabriel Merino, Miguel A. Mndez-Rojas, Hiram I. Beltrn, Clemence Corminboeuf, Thomas Heine, and Alberto Vela

J. Am. Chem. Soc., **2004**, 126 (49), 16160-16169• DOI: 10.1021/ja047848y • Publication Date (Web): 19 November 2004

HOMO

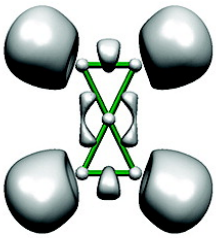

ELF

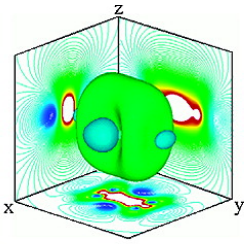

Induced Magnetic Field

More About This Article

Additional resources and features associated with this article are available within the HTML version:

- Supporting Information
- Links to the 14 articles that cite this article, as of the time of this article download
- Access to high resolution figures
- Links to articles and content related to this article
- Copyright permission to reproduce figures and/or text from this article

View the Full Text HTML

J|A|C|S
ARTICLES
Published on Web 11/19/2004

Theoretical Analysis of the Smallest Carbon Cluster Containing a Planar Tetracoordinate Carbon

Gabriel Merino,*[,†,#] Miguel A. Méndez-Rojas,[‡] Hiram I. Beltrán,[§] Clemence Corminboeuf,[¶] Thomas Heine,[†] and Alberto Vela*[,#]

Contribution from the Institut für Physikalische Chemie und Elektrochemie, TU Dresden, D-01062 Dresden, Germany, Departamento de Química y Biología, Universidad de las Américas-Puebla, Ex-Hda. de Sta. Catarina Mártir, A. P. 100, Cholula 72820, Puebla, Mexico, Instituto Mexicano del Petróleo, Eje Central Lázaro Cárdenas 152, México, D. F. 07730, Mexico, Université de Genève 30, quai Ernest-Ansermet, CH-1211 Geneva 4, Switzerland, and Departamento de Química, Centro de Investigación y de Estudios Avanzados, A. P. 14-740, México, D.F. 07000, Mexico

Received April 14, 2004; E-mail: Gabriel.Merino@chemie.tu-dresden.de (G.M.); avela@mail.cinvestav.mx (A.V.)

Abstract: A series of molecules, based on the smallest carbon cluster with one planar tetracoordinate carbon atom, C_5^{2-}, are presented. To gain a better understanding about which electronic factors contribute to their stabilization, several global reactivity indexes, molecular scalar fields, and magnetic responses were calculated. The optimized bond lengths and the topological analysis of the electron density show that the central carbon atom in the parent dianion C_5^{2-} has a planar local environment, and it is coordinated to four other carbon atoms. The bonding of the parent dianion with the metal cations is highly ionic. The magnetic properties show that the C_5^{2-} derivatives are strongly diatropic and have a remarkable transferability of structural and electronic features from the anion to the salts. The theoretical analysis suggests that the lithium salt, C_5Li_2, is the most plausible candidate for experimental detection.

Introduction

In 1874, van't Hoff and LeBel postulated one of the most important paradigms of organic chemistry: the tetrahedral carbon atom.[1,2] This seminal contribution gave meaning to numerous chemical concepts, such as chirality and stereoisomerism. More than a century after van't Hoff and LeBel's proposal, Hoffmann, Alder, and Wilcox discussed the electronic conditions under which a planar tetracoordinate carbon (ptC) atom could exist.[3] When methane has a planar D_{4h} structure, the central carbon atom takes an sp^2 hybridization, with one lone pair orthogonal to the molecular plane. Therefore, only six electrons occupy bonding orbitals (Figure 1), contrasting with the four bonding pairs present in tetrahedral T_d methane. Hoffmann et al. suggested that to stabilize a molecule containing a ptC, it is necessary to include the lone pair in the bonding framework by replacing one or more hydrogen atoms with good σ-donor/π-acceptor ligands or by incorporating the lone pair into a $(4n + 2)\pi$ delocalized system. Inspired by this mechanism, several molecules with a ptC have been successfully predicted and even experimentally characterized. The smallest possible (pentaatomic) tetracoordinate planar carbon-containing molecules, with ligands different from carbon, were proposed by Boldyrev and Schleyer in 1991[4] and were experimentally realized by Wang and Boldyrev.[5] It is worthwhile to mention that all of these structures, which are stabilized by an electronic mechanism, share a common feature: they have at least one atom, different to carbon, that is bonded to the ptC.[4,6−27]

† Institut für Physikalische Chemie und Elektrochemie.
‡ Universidad de las Américas-Puebla.
§ Instituto Mexicano del Petróleo.
¶ Université de Genève.
# Centro de Investigación y de Estudios Avanzados.

(1) van't Hoff, J. H. *Arch. Neerl. Sci. Exactes Nat.* **1874**, 445−454.
(2) LeBel, J. A. *Bull. Soc. Chim. Fr.* **1874**, 22.
(3) Hoffmann, R.; Alder, R. W.; Wilcox, C. F. *J. Am. Chem. Soc.* **1970**, *92*, 4992−4993.
(4) Schleyer, P. v. R.; Boldyrev, A. I. *J. Chem. Soc., Chem. Commun.* **1991**, 1536−1538.
(5) Wang, L. S.; Boldyrev, A. I.; Li, X.; Simons, J. *J. Am. Chem. Soc.* **2000**, *122*, 7681−7687.
(6) Collins, J. B.; Dill, J. D.; Jemmis, E. D.; Apeloig, Y.; Schleyer, P. v. R.; Seeger, R.; Pople, J. A. *J. Am. Chem. Soc.* **1976**, *98*, 5419−5427.
(7) Crans, D. C.; Snyder, J. P. *J. Am. Chem. Soc.* **1980**, *102*, 7152−7154.
(8) Chandrasekhar, J.; Wurthwein, E. U.; Schleyer, P. v. R. *Tetrahedron* **1981**, *37*, 921−927.
(9) Jemmis, E. D. *Curr. Sci.* **1983**, *52*, 1049−1053.
(10) Boldyrev, A. I.; Simons, J. *J. Am. Chem. Soc.* **1998**, *120*, 7967−7972.
(11) Erker, G.; Rottger, D. *Angew. Chem., Int. Ed. Engl.* **1993**, *32*, 1623−1625.
(12) Gunale, A.; Steiner, D.; Schweikart, D.; Pritzkow, H.; Berndt, A.; Siebert, W. *Chem. Eur. J.* **1998**, *4*, 44−52.
(13) Merschrod, E. F.; Tang, S. H.; Hoffmann, R. *Z. Naturforsch., B* **1998**, *53*, 322−332.
(14) Radom, L.; Rasmussen, D. R. *Pure Appl. Chem.* **1998**, *70*, 1977−1984.
(15) Erker, G. *Chem. Soc. Rev.* **1999**, *28*, 307−314.
(16) Gribanova, T. N.; Minyaev, R. M.; Minkin, V. I. *Collect. Czech. Chem. Commun.* **1999**, *64*, 1780−1789.
(17) Li, X.; Wang, L. S.; Boldyrev, A. I.; Simons, J. *J. Am. Chem. Soc.* **1999**, *121*, 6033−6038.
(18) Siebert, W.; Gunale, A. *Chem. Soc. Rev.* **1999**, *28*, 367−371.
(19) Boldyrev, A. I.; Li, X.; Wang, L. S. *Angew. Chem., Int. Ed.* **2000**, *39*, 3307−3310.
(20) Choukroun, R.; Donnadieu, B.; Zhao, J. S.; Cassoux, P.; Lepetit, C.; Silvi, B. *Organometallics* **2000**, *19*, 1901−1911.
(21) Exner, K.; Schleyer, P. v. R. *Science* **2000**, *290*, 1937−1940.
(22) Li, X.; Zhang, H. F.; Wang, L. S.; Geske, G. D.; Boldyrev, A. I. *Angew. Chem., Int. Ed.* **2000**, *39*, 3630−3633.
(23) Boldyrev, A. I.; Wang, L. S. *J. Phys. Chem. A* **2001**, *105*, 10759−10775.
(24) Wang, Z. X.; Manojkumar, T. K.; Wannere, C.; Schleyer, P. v. R. *Org. Lett.* **2001**, *3*, 1249−1252.

10.1021/ja047848y CCC: $27.50

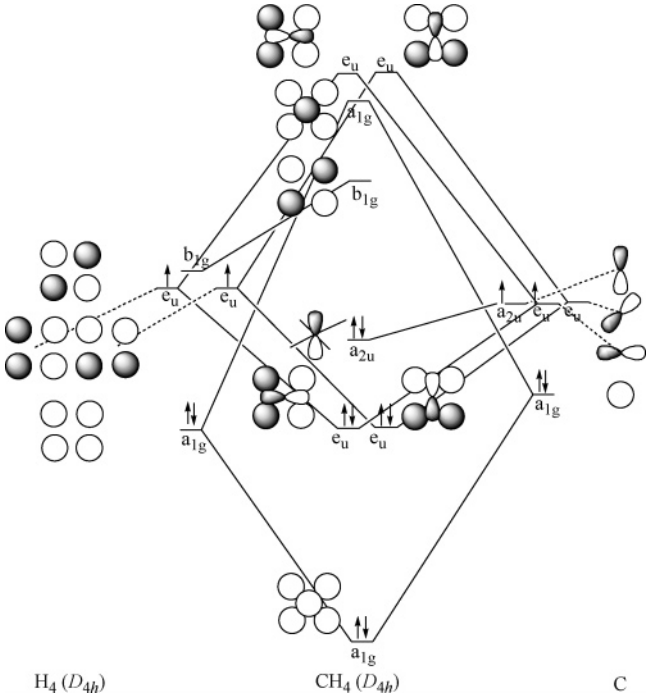

Figure 1. Schematic molecular orbital diagram of planar methane with D_{4h} symmetry.

Another approach for stabilizing a ptC is to impose geometrical constraints that force the central carbon atom and its nearest neighbors to be in a plane. This mechanical approach can be achieved by building a cage around the ptC, as it has been done in the alkaplanes.[14,28,29] Hitherto, the experimental efforts done to isolate one of these mechanically stabilized molecules containing a ptC have been unfruitful. The lack of success may be due to the fact that the p-orbital normal to the ptC plane, generally the HOMO, is strongly localized on the central carbon atom, resulting in a cage that is held together by very weak forces that prevent its stabilization and, hence, its experimental isolation.

In 1997, Keese stated that "*...despite considerable computational efforts, no structures with a planar tetracoordinate C(C)$_4$ have been found*".[30] Two years later, Rasmussen and Radom reported the first mechanically stabilized ptC with a C(C)$_4$ skeleton [ptC(C)$_4$], the dimethanospiro[2,2]octaplane.[29] After this work, Wang and Schleyer designed a set of boron bisubstituted spiroalkanes with a ptC(C)$_4$, which is stabilized by both strategies, mechanical and electronic.[31,32] In a recent communication, the first family of molecules based on a C_5^{2-} skeleton that successfully stabilized a ptC(C)$_4$ only by electronic factors was reported.[33] More recently, Minyaev et al. designed a family of cage structures with a half-ptC(C)$_4$ center,[34] while Priyakumar et al. proposed a benzene dication isomer with three ptC(C)$_4$'s.[35]

The motivation of the current work is to present a series of molecules containing one ptC(C)$_4$ and to discuss, in detail, the electronic requirements for their stabilization. After examining the potential energy surface (PES) of C_5^{2-}, we propose several metallic salts with a ptC(C)$_4$. The electronic stabilization and the bonding scheme are analyzed through the study of various reactivity indexes[36] and molecular scalar fields (the electron density, $\rho(\mathbf{r})$,[37] the electron localization function, ELF($\mathbf{r}$),[38,39] and the molecular orbitals, $\{\phi(\mathbf{r})\}$). The magnetic properties of these compounds are studied, giving particular attention to the nucleus-independent chemical shifts (NICS)[40] of all the molecular systems considered and the induced magnetic field of C_5^{2-}, C_5Li^-, and C_5Li_2.

Computational Details

The geometry optimizations and electronic structure calculations were performed using Gaussian 98.[41] Structures were optimized using Becke's exchange (B),[42] Lee, Yang, and Parr (LYP) correlation,[43] and within the hybrid functional (B3LYP) approach, as implemented in Gaussian. All calculations were done using the 6-311++G(2d) basis set.[44] Reoptimization of C_5^{2-} using the same hybrid functional, the full second-order Møller−Plesset (MP2),[45] and the frozen-core coupled cluster, including single, double, and noniteratively triple excitations [CCSD(T)][46] with the 6-311++G(2df) basis set, results in unsubstantial modifications of the structure (Figure 2). Therefore, one can assume that the hybrid approach, B3LYP, with the basis set used in this work, is a reasonable chemical model for studying the molecular structures associated to the C_5^{2-} fragment. Every stationary point on the PES was characterized by a harmonic analysis using the same theoretical methodology as that used in the optimization. The harmonic frequencies were used to evaluate the zero-point energy correction with a scaling of corrections (scaled by 0.9806, as recommended by Scott and Radom).[47] Minima connected by a given transition state were confirmed by intrinsic reaction coordinate (IRC) calculations.[48] To gain further understanding of the chemical bonding in the ptC(C)$_4$, the electronic density and the electron localization function were analyzed with the

(25) Sahin, Y.; Prasang, C.; Hofmann, M.; Subramanian, G.; Geiseler, G.; Massa, W.; Berndt, A. *Angew. Chem., Int. Ed.* **2003**, *42*, 671−674.
(26) Huang, J. H.; Luci, J. J.; Lee, T. Y.; Swenson, D. C.; Jensen, J. H.; Messerle, L. *J. Am. Chem. Soc.* **2003**, *125*, 1688−1689.
(27) Li, S.-D.; Ren, G.-M.; Miao, C.-Q.; Jin, Z.-H. *Angew. Chem., Int. Ed.* **2004**, *43*, 1371−1373.
(28) McGrath, M. P.; Radom, L. *J. Am. Chem. Soc.* **1993**, *115*, 3320−3321.
(29) Rasmussen, D. R.; Radom, L. *Angew. Chem., Int. Ed.* **1999**, *38*, 2876−2878.
(30) Thommen, M.; Keese, R. *Synlett* **1997**, 231−240.
(31) Wang, Z. X.; Schleyer, P. v. R. *J. Am. Chem. Soc.* **2001**, *123*, 994−995.
(32) Wang, Z. X.; Schleyer, P. v. R. *J. Am. Chem. Soc.* **2002**, *124*, 11979−11982.
(33) Merino, G.; Mendez-Rojas, M. A.; Vela, A. *J. Am. Chem. Soc.* **2003**, *125*, 6026−6027.
(34) Minyaev, R. M.; Minkin, V. I.; Gribanova, T. N.; Starikov, A. G.; Hoffmann, R. *J. Org. Chem.* **2003**, *68*, 8588−8594.
(35) Priyakumar, U. D.; Reddy, A. S.; Sastry, G. N. *Tetrahedron Lett.* **2004**, *45*, 2495−2498.
(36) Geerlings, P.; De Proft, F.; Langenaeker, W. *Chem. Rev.* **2003**, *103*, 1793−1874.
(37) Bader, R. F. W. *Atoms in Molecules: A Quantum Theory*; Oxford University Press: Oxford, 1990.
(38) Savin, A.; Nesper, R.; Wengert, S.; Fassler, T. F. *Angew. Chem., Int. Ed. Engl.* **1997**, *36*, 1809−1832.
(39) Becke, A. D.; Edgecombe, K. E. *J. Chem. Phys.* **1990**, *92*, 5397−5403.
(40) Schleyer, P. v. R.; Maerker, C.; Dransfeld, A.; Jiao, H. J.; Hommes, N. *J. Am. Chem. Soc.* **1996**, *118*, 6317−6318.
(41) Frisch, M. J.; Trucks, G. W.; Schlegel, H. B.; Scuseria, G. E.; Robb, M. A.; Cheeseman, J. R.; Zakrzewski, V. G.; Montgomery, J. A.; Stratmann, R. E.; Burant, J. C.; Dapprich, S.; Millan, J. M.; Daniels, A. D.; Kudin, K. N.; Strain, M. C.; Farkas, O.; Tomasi, J.; Barone, V.; Cossi, M.; Cammi, R.; Mennucci, B.; Pomelli, C.; Adamo, C.; Clifford, S.; Ochterski, J.; Petersson, G. A.; Ayala, P. Y.; Cui, Q.; Morokuma, K.; Malick, D. K.; Rabuck, A. D.; Raghavachari, K.; Foresman, J. B.; Cioslowski, J.; Ortiz, J. V.; Baboul, A. G.; Stefanov, B. B.; Liu, G.; Liashenko, A.; Piskorz, P.; Komaromi, I.; Gomperts, R.; Martin, R. L.; Fox, D. J.; Keith, T.; Al-Laham, M. A.; Peng, C. Y.; Nanayakkara, A.; Gonzales, C.; Challacombe, M.; Gill, P. M. W.; Johnson, B.; Chen, W.; Wong, M. W.; Andreas, J. L.; Head-Gordon, M.; Reploge, E. S.; Pople, J. A. *Gaussian 98*, revision A7; Gaussian Inc.: Pittsburgh, PA, 1998.
(42) Becke, A. D. *J. Chem. Phys.* **1993**, *98*, 5648−5652.
(43) Lee, C. T.; Yang, W. T.; Parr, R. G. *Phys. Rev. B* **1988**, *37*, 785−789.
(44) Krishnan, R.; Binkley, J. S.; Seeger, R.; Pople, J. A. *J. Chem. Phys.* **1980**, *72*, 650−654.
(45) Møller, C.; Plesset, M. S. *Phys. Rev.* **1934**, *46*, 618−622.
(46) Pople, J. A.; Head-Gordon, M.; Raghavachari, K. *J. Chem. Phys.* **1987**, *87*, 5968−5975.
(47) Scott, A. P.; Radom, L. *J. Phys. Chem.* **1996**, *100*, 16502−16513.
(48) Fukui, K. *Acc. Chem. Res.* **1981**, *14*, 363−368.

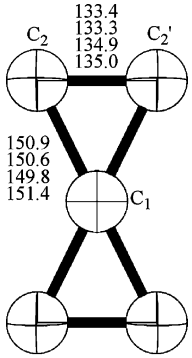

1

Figure 2. Optimized geometry of the parental skeleton C_5^{2-}. From top to bottom, the bond lengths correspond to B3LYP/6-311++G(2d), B3LYP/6-311++G(2df), MP2(full)/6-311++G(2df), and CCSD(T)(frozen core)/6-311++G(2df), respectively.

AIM2000[49] and TopMod[50] programs, using the density matrixes obtained from the corresponding Gaussian calculations. ^{13}C NMR chemical shifts, NICS, and HOMO−NICS were computed using a gauge, including atomic orbitals (GIAO)[51] at the PW91/6-311++G-(2d)//B3LYP/6-311++(2d), employing the MAG-Respect program.[52] The ^{13}C NMR chemical shifts were referenced to TMS (calculated absolute shift at the same level of theory, i.e., σ(C) = 182.6 part per million (ppm)). The induced magnetic field of C_5^{2-} was performed using PW91/IGLO-II and PW91/IGLO-III,[53] while for C_5Li^- and C_5Li_2, only the former theoretical methodology was used. For the other metals, the calculations leading to the rendering of the induced magnetic field were not done. It is to be expected that they should not be very different from those selected here. The shielding tensors were computed using the IGLO method.[54] The deMon 2002 program[55] was used to compute the molecular orbitals, and the deMon-NMR package[56] was used for the shielding tensors. Induced magnetic fields were computed in ppm of the external fields. When an external magnetic field of $|\vec{B}_{ext}| = 1$ T is assumed, the unit of the induced field is 1.0 μT, which is equivalent to 1.0 ppm of the shielding tensor. For the rendering of the induced magnetic fields, the molecules were oriented in the following way. The center of mass is located at the origin of the coordinate system with the *z*-axis parallel to the highest order symmetry axis of the molecule. The external field is applied perpendicular to the molecular plane. VU[57] and Molekel[58] were employed for the visualization of the molecular fields.

Results and Discussion

Structure and Energetics. The smallest possible cluster containing a C(C)$_4$ skeleton is C_5. Experimental and theoretical studies show that the linear structure of the neutral species is energetically favored, and no evidence of planar isomers of C_5 containing a ptC is available.[59,60] Thus, it is tempting to consider the possibility of extracting or adding electrons and to scan the PES of these ions aiming to find a C_5 cluster containing a ptC. To illustrate this, consider the neutral D_{2h} structure, which has three imaginary frequencies. After removing two electrons, one finds a stationary point with two imaginary frequencies. On the other hand, the addition of two electrons generates a local minimum having the desired ptC(C)$_4$ atom. This D_{2h} optimized geometry of C_5^{2-} (**1**) is shown in Figure 2. Note that the C_1-C_2 bond length (150.9 pm) is comparable with those calculated for dimethanospiro[2.2]octaplane (150.4 pm)[29] and several [4.4.4.5]fenestrene derivatives (149.3−152.9 pm).[61]

Considering that the experimental observation of C_5^{2-} strongly depends on the topography of the PES, an extensive exploration of this hypersurface was performed (Figure 3). It can be seen that only four structures are local minima on the PES, including **1**. Two of them (**1A** and **1B**) are lower in energy than **1** (202.4 and 184.8 kJ mol^{-1}, respectively), whereas the three-dimensional D_{3h} structure, **1C**, is 179.5 kJ mol^{-1} higher in energy. Structure **1D** is the transition state involved in the rearrangement that isomerizes **1B** into **1**. It should be noted that structure **1D** is not planar and lies very close in energy to **1** (12.6 kJ mol^{-1}). The **1E**−**1H** structures have one imaginary frequency, and they are not connected to the ptC-containing molecule. The rest of the stationary points found on the PES of C_5^{2-} are higher-order saddle points. It is worth noting that the MP2 and CCSD(T) calculations of the local minimum **1** confirm the stability of the dianion, supporting the results obtained with the hybrid exchange−correlation density functional.

Due to the large negative charge, one expects that C_5^{2-} must have electrons that are easily detachable from the structure. The positive values for the energies of some occupied molecular orbitals confirm the existence of these unbounded electrons. The HOMO (4.28 eV) and four other occupied MOs of **1** have positive eigenvalues. This should not be very surprising since the HOMOs of dianions, such as CAl_4^{2-} and CB_6^{2-}, also have positive orbital energies (3.02 and 4.17 eV, respectively, at the same level of theory).[17,21] Clearly, to have any chance of suggesting a detectable structure, it is mandatory to stabilize (lower) these orbital energies. One possibility is to introduce positive charges into the parent dianion, as was done with CAl_4^{2-}, which after being dressed by a sodium cation, the resulting anion was stable enough to be studied by photoelectron spectroscopy (see ref 22). In our case, the resulting compounds with one and two metals C_5M^n ($n = 1-, 0$) (**2**) and $C_5M_2^n$ ($n = 0, 2$) (**3**) are depicted in Figure 4. Notice that the addition of the cations does not destroy the planarity of the molecules. The bare C_5^{2-} ion (**1**) and **3** have D_{2h} symmetry, while **2** belongs to a C_{2v} point group. The harmonic analysis of these molecular structures reveals that they are local minima on the corresponding PES (Table 1).

As can be seen in Table 1, adding one counterion with a formal charge of +1 (M = Li, Na, K, Cu) does not change the planarity of the structure. C_5K^- has the largest increase in the C_1-C_2 bond length (only 1.7 pm), while C_5Na^- shows a reduction in the C_1-C_2' distance (2.0 pm). The geometrical deformations are more pronounced when one dication is incorporated in the structure. The extreme situation corresponds

(49) Biegler-Konig, F.; Schonbohm, J.; Bayles, D. *J. Comput. Chem.* **2001**, *22*, 545−559.
(50) Noury, S.; Krokidis, X.; Fuster, F.; Silvi, B. *TopMoD*; Universite Pierre et Marie Curie: Paris, 1997.
(51) Corminboeuf, C.; Heine, T.; Weber, J. *Phys. Chem. Chem. Phys.* **2003**, *5*, 246−251.
(52) Malkin, V. G.; Malkina, O. L.; Reviakine, R.; Schimmelpfennig, B.; Arbuznikov, V.; Kaupp, M. *MAG-ReSpect*, version 1.0; 2001.
(53) Kutzelnigg, W.; Fleischer, U.; Schindler, M. *The IGLO-Method: Ab Initio Calculation and Interpretation of NMR Chemical Shifts and Magnetic Susceptibilities*; Springer-Verlag: Heidelberg, Germany, 1990.
(54) Kutzelnigg, W. *Isr. J. Chem.* **1980**, *19*, 193−200.
(55) Koster, A. M.; Geudtner, G.; Goursot, A.; Heine, T.; Vela, A.; Salahub, D. R. *deMon 2001*; NRC: Ottawa, Canada, 2002.
(56) Malkin, V. G.; Malkina, O. L.; Salahub, D. R. *Chem. Phys. Lett.* **1993**, *204*, 80−86.
(57) Ozell, B.; Camarero, R.; Garon, A.; Guibault, F. *Finite Elem. Anal. Des.* **1995**, *19*, 295.
(58) Portmann, S.; Luthi, H. P. *Chimia* **2000**, *54*, 766−770.
(59) Bernath, P. F.; Hinkle, K. H.; Keady, J. J. *Science* **1989**, *244*, 562−564.
(60) Dua, S.; Bowie, J. H. *J. Phys. Chem. A* **2002**, *106*, 1374−1380.
(61) Rao, V. B.; George, C. F.; Wolff, S.; Agosta, W. C. *J. Am. Chem. Soc.* **1985**, *107*, 5732−5739.

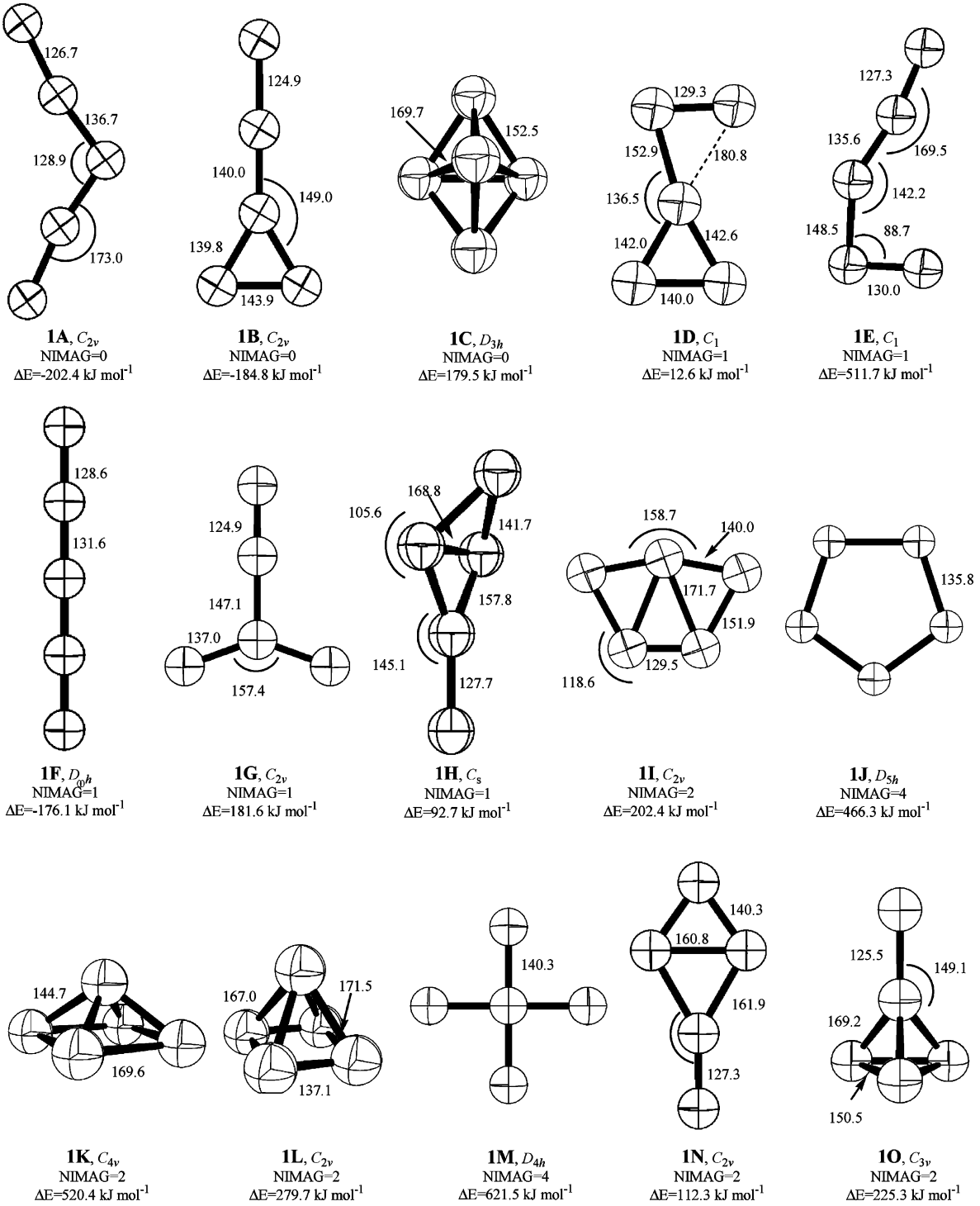

Figure 3. Stationary points of the C_5^{2-} skeleton calculated with B3LYP/6-311++G(2d). NIMAG is the number of imaginary harmonic frequencies obtained for each structure using the same methodology, and ΔE is the energy difference of the corresponding structure minus that of **1**, including the scaled ZPE (0.98). All distances are in picometers and angles in degrees.

to C_5Zn (see Table 1), where the C_1-C_2 distance increases by 5.0 pm and the C_1-C_2' distance decreases by 6.0 pm. The inclusion of two metal cations produces a reduction of the C_1-C_2 bond lengths from 0.3 (C_5K_2) to 4.8 pm ($C_5Zn_2^2$). Furthermore, the C_2-C_2' bond lengths remain practically unchanged after the insertion of one or two metal ions.

Molecular Orbital Analysis. It has been customary to discuss the stability of ptC-containing systems in terms of the nature of the frontier molecular orbitals (FMO), the HOMO, and the LUMO. For instance, in the case of methane, the transformation that changes T_d CH_4 into a D_{4h} planar structure breaks the 3-fold degeneracy of the t_2 MOs, producing one set of 2-fold degenerate e_u MOs and one a_{2u} MO, the HOMO of planar methane. This last MO is a nonbonding pure p-orbital perpendicular to the molecular plane. Clearly, this reshuffle of the electron density reduces the bond order of the molecule, but more important, it is the fact that the D_{4h} stationary point is not even a transition state in the PES of methane; it is a higher-

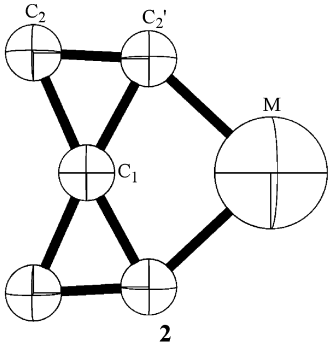

2

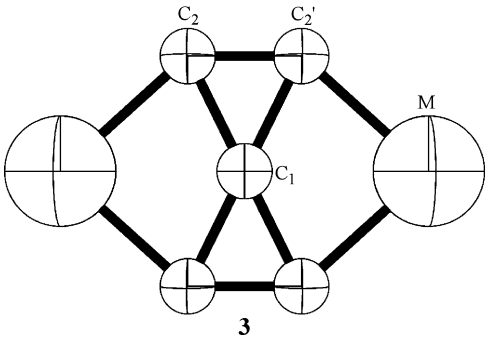

3

Figure 4. Schematic representation and atom labeling of the C_5M and C_5M_2 structures, where M is a metal cation.

Table 1. Selected Bond Lengths (in picometers), Angles (in degrees), and Smallest Frequencies (in cm^{-1}) of **1**−**3**

	M	*n*	C_1–C_2	C_1–C_2'	C_2–C_2'	C_2'–M	C_2–C_1–C_2	C_2–C_1–C_2'	frequency
1		2−	150.9		133.4		127.5		168.3
2	Li	1−	151.7	150.6	133.0	193.0	132.4	123.1	218.8
	Na	1−	152.5	148.7	132.8	230.5	130.7	124.7	157.4
	K	1−	152.6	149.0	132.8	261.4	128.2	127.3	120.0
	Cu	1−	150.8	150.3	133.0	200.2	141.8	113.4	201.5
	Be	0	154.7	149.2	132.8	162.4	141.3	115.1	235.4
	Mg	0	155.3	146.1	132.1	205.3	136.8	119.5	186.9
	Ca	0	154.2	148.2	132.9	225.0	129.6	126.3	174.3
	Zn	0	155.9	144.9	131.6	203.6	142.0	114.6	161.7
3	Li	0	150.1		132.8	200.6	127.5		172.3
	Na	0	150.0		132.7	235.1	127.5		81.7
	K	0	150.6		132.7	266.8	127.7		52.9
	Cu	0	148.9		133.4	207.8	126.8		85.6
	Be	2	148.5		133.3	177.0	126.6		195.4
	Mg	2	148.2		132.6	215.4	126.9		131.4
	Ca	2	149.9		132.3	239.7	127.6		103.8
	Zn	2	146.1		132.5	214.1	126.1		65.4

order saddle point.[62] However, the MO analysis of planar methane is a valuable guiding light to search for mechanisms that can produce compounds with the desired ptCs. One strategy to stabilize electronically a ptC moiety is to substitute the hydrogen atoms with σ-donor elements (e.g., boron and lithium). Another alternative is to delocalize the p-orbital over the ptC skeleton (i.e., to transform it into a bonding orbital). As depicted in Figure 5, this is the case of C_5^{2-}. The $1b_{3u}$ MO, which has an important contribution from the p-orbital of the central carbon atom, is the lowest-lying π-orbital of the carbon framework. It covers completely the $C(C)_4$ skeleton and together with the next occupied π-orbital, the $1b_{2g}$ MO, contributes to the double-bond character of the C_2−C_2' bond. This delocalization of the p-orbital is one of the fundamental reasons to understand the stability of the C_5^{2-} structure.

(62) Gordon, M. S.; Schmidt, M. W. *J. Am. Chem. Soc.* **1993**, *115*, 7486−7492.

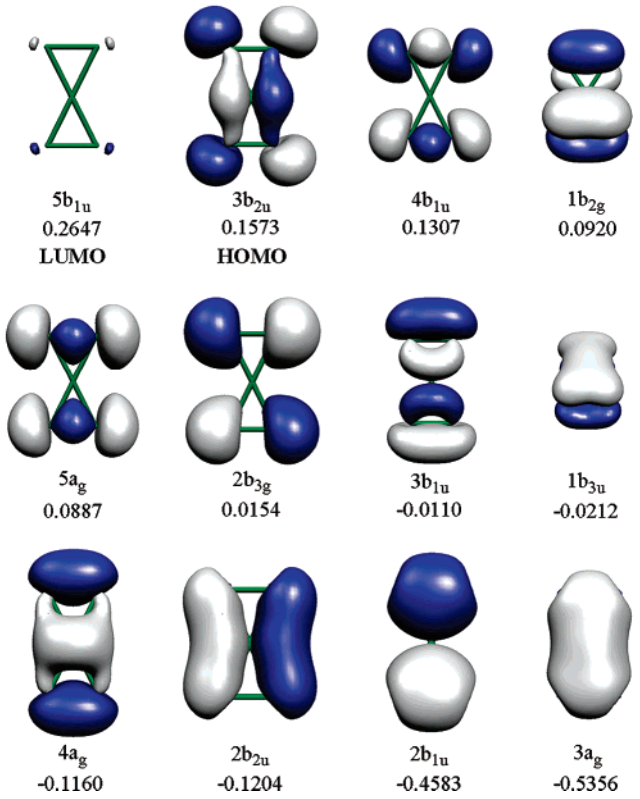

Figure 5. B3LYP molecular orbitals and orbital energies (in atomic units) of C_5^{2-}. The structure belongs to the D_{2h} point group. The value of the isosurface is 0.05 au.

Table 2. HOMO, LUMO, Hardness (η), Electronegativity (χ), Electrophilicity (ω), and Natural Bond Orbital Charges (Q)[a]

	M	*n*	HOMO	LUMO	η	χ	ω	Q_{ptC}	Q_M
1		2−	0.1573	0.2657	0.1074	−0.2115	0.2072	−0.27	
2	Li	1−	−0.0225	0.0596	0.0822	−0.0186	0.0021	−0.25	0.76
	Na	1−	−0.0126	0.0465	0.0591	−0.0170	0.0024	−0.24	0.69
	K	1−	−0.0038	0.0397	0.0435	−0.0179	0.0037	−0.25	0.74
	Cu	1−	−0.0307	0.0579	0.0886	−0.0136	0.0010	−0.19	0.60
	Be	0	−0.2551	−0.1128	0.1424	0.1839	0.1188	−0.20	1.45
	Mg	0	−0.2210	−0.1460	0.0750	0.1835	0.2245	−0.20	1.37
	Ca	0	−0.1961	−0.1071	0.0889	0.1516	0.1292	−0.25	1.60
	Zn	0	−0.2413	−0.1635	0.0777	0.2024	0.2635	−0.15	1.12
3	Li	0	−0.2057	−0.0403	0.1654	0.1230	0.0457	−0.29	0.87
	Na	0	−0.1732	−0.0400	0.1332	0.1066	0.0427	−0.25	0.87
	K	0	−0.1495	−0.0304	0.1191	0.0899	0.0340	−0.25	0.90
	Cu	0	−0.2131	−0.0910	0.1220	0.1521	0.0947	−0.24	0.76
	Be	2	−0.6928	−0.5367	0.1560	0.6148	1.2114	−0.41	1.67
	Mg	2	−0.5854	−0.4357	0.1497	0.5106	0.8707	−0.28	1.74
	Ca	2	−0.5297	−0.3711	0.1586	0.4504	0.6395	−0.28	1.82
	Zn	2	−0.6301	−0.5074	0.1227	0.5688	1.3184	−0.26	1.50

[a] All quantities are in atomic units.

Global Reactivity Indexes. The FMO energies, together with some global reactivity indexes, are presented in Table 2. These indexes have been calculated within the finite differences approximation and using Koopmans' theorem.[36] The first noticeable feature is that the FMO energies of C_5^{2-} are both positive. This might not be too surprising since it must be very likely that this parental dianion has a natural tendency to give away its electrons. Interestingly, the addition of one singly positive cation (alkaline or transition metal) is enough to bring the energies of the HOMOs to negative values, but the LUMOs of these C_5M^- species preserve its unbound character. The substitution of one singly positive metal cation with a doubly positive ion or the addition of a second cation brings the FMO

energies to negative values. As expected, the higher the formal charge of the structure, the lower the orbital energies (i.e., they are more negative for $C_5M_2^2$). From the values reported in Table 2, one can see that for the parental skeleton C_5^{2-}, as well as for the structures with only one singly charged metal, the electronegativity is negative. This indicates that the parental dianion has a very high tendency to give away electrons. On the other hand, from the neutral species, C_5M or C_5M_2, to the doubly positive ones, the electronegativity is positive. Therefore, the addition of metal cations lowers the tendency of the corresponding salt to give away their electrons. Notice that for a given total charge (2−, 1−, 0, 2), the values of the electronegativity are not very sensitive to the type of metal cation substituted in the C_5^{2-} skeleton. The analysis of the global hardness sheds more light on the stability of these ptC-containing structures. With the sole exception of C_5Be, the addition of a single metal cation enhances the softness of the molecule, or in other words, C_5^{2-} is harder than $C_5M^{(1-,0)}$. On the contrary, when two metal cations (singly or doubly charged) are present, the resulting structure, $C_5M_2^{(0,2)}$, is harder than the parental moiety. It is interesting to note that the hardest species found is the doubly substituted lithium compound. Finally, the electrophilicity[63] shows that $C_5M_2^2$ has a very high tendency to lower its energy by accepting electrons, followed by the alkaline earth monosubstituted neutral compounds. The electrophilicity of the parental skeleton, C_5^{2-}, is almost equal to that of the latter species, but since it is negatively charged, the tendency of this species is to give away electrons, which is in full agreement with the fact that it has a negative electronegativity. In summary, the global reactivity indexes show that the parental structure, C_5^{2-}, is a hard base with a high tendency to give away its electrons. This dianion reacts with hard acids, such as the lithium cation, to produce hard salts, the doubly substituted $C_5M_2^{(0,2)}$ compounds, which are good candidates for experimental observation.

Topological Analysis of the Electron Density. To gain further insight into the bonding mechanism prevailing in the molecules considered in this work, a topological analysis of the electron density was done.[37] From the molecular graph depicted in Figure 6a, one can see that the central carbon atom in the C_5^{2-} skeleton is connected to its four neighbor carbon atoms by a gradient path. This nonempirical connectivity, together with the bond distances obtained for this structure, strongly supports the tetracoordination of the central carbon atom. For all of the structures studied, there is a gradient path connecting the C_2 and C_2' atoms. From the values of the descriptors reported in Table 3, it can be concluded that C_1 is bonded to C_2 by a weak covalent single bond, while the bond that connects C_2 with C_2' is a double bond. This bonding picture is in line with the bond lengths found for this structure and with the MO analysis presented in the previous sections. The significant curvature exhibited by the gradient paths, which connect the ptC (carbon C_1) with the external carbon atoms, as well as the large ellipticity, points toward the existence of multicenter bonds.

In the metal-containing systems, the molecular connectivity depends on the charge of the counterion. After one singly charged cation is added to the C_5^{2-} skeleton, the central carbon atom preserves its connectivity (Figure 6b), indicating that the electron distribution of the parental dianion is not significantly perturbed. In contrast, the topology of the electron density for neutral C_5M shows important changes. The most relevant difference with respect to the C_5M^- structures is that there is no gradient path between C_1 and C_2 (Figure 6c). This is in agreement with the geometry changes induced by the addition of doubly charged cations. Thus, the molecular graphs of the C_5M systems (M = Be, Mg, Ca, Zn) suggest that in these molecules, the C_1 atom is no longer tetracoordinated. Independently of their charges, the introduction of two metallic ions in the long sides of the rectangle results in a molecular graph that preserves the topological characteristics of the C_5^{2-} moiety, as it is depicted in Figure 6d.

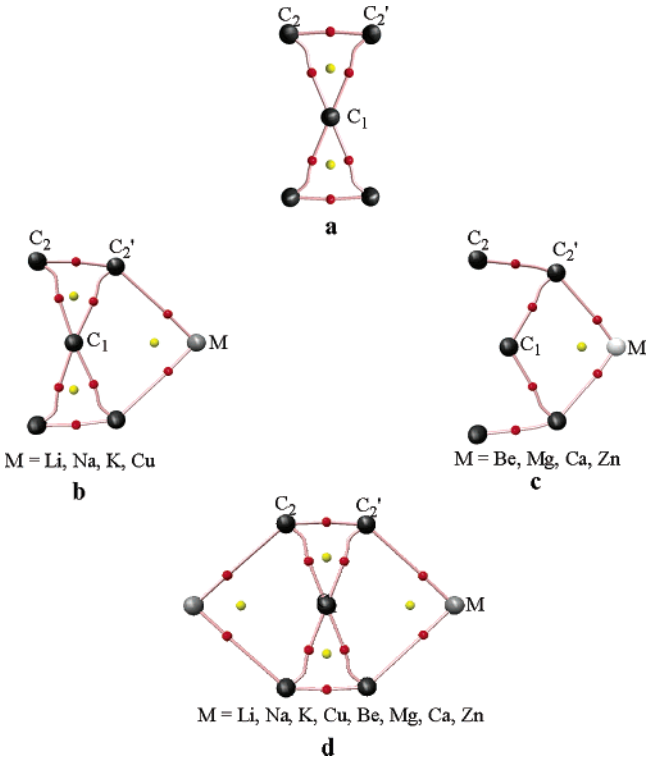

Figure 6. Molecular graphs of (a) C_5^{2-}, (b) C_5M^-, (c) C_5M, and (d) $C_5M^{(0,2)}$, where M is the metal cation indicated at the bottom of the corresponding graph. The red and yellow spheres correspond to bond and ring critical points, respectively. The attractors (nuclei) are shown as black spheres for carbon and gray spheres for the metal cations.

The bonding picture that emerges from the chemical reactivity indexes and from the topological analysis of the electron density is that the parental C_5^{2-} skeleton binds to the alkaline and alkaline earth atoms by a highly ionic bond with a remarkable transferability of properties from the isolated dianion to the C_5M_2 salts. The NBO charges[64] reported in Table 2, as well as the positive values of the Laplacian (Table 3) of the electron density corresponding to the C_2'−M critical points, provide further support to this bonding mechanism.

Analysis with the ELF. Another key question to understand the stability of ptC-containing molecules is the nature of the lone pair located in the central carbon atom. The topology of the electron density provides a consistent mapping to bonding models, but unless it is supplied with additional input, like the Laplacian of the electron density, it does not provide information

(63) Parr, R. G.; von Szentpaly, L.; Liu, S. B. *J. Am. Chem. Soc.* **1999**, *121*, 1922−1924.

(64) Reed, A. E.; Curtiss, L. A.; Weinhold, F. *Chem. Rev.* **1988**, *88*, 899−926.

Table 3. Descriptors from the Topological Analysis of the Electronic Density of **1**−**3**[a]

			C_1–C_2			C_1–C_2'			C_2–C_2'			C_2–M		
	M	*n*	ρ	*L*	ϵ	ρ	*L*	ϵ	ρ	*L*	ϵ	ρ	*L*	ϵ
1		2−	0.220	0.030	1.209				0.354	0.272	0.011			
2	Li	1−	0.217	0.019	1.722	0.224	0.031	1.160	0.355	0.275	0.015	0.039	−0.055	0.493
	Na	1−	0.214	0.004	2.624	0.230	0.046	0.874	0.357	0.278	0.011	0.028	−0.037	0.206
	K	1−	0.215	0.005	2.528	0.228	0.043	0.938	0.359	0.280	0.012	0.028	−0.026	0.138
	Cu	1−	0.220	0.029	1.435	0.225	0.031	1.081	0.350	0.266	0.008	0.090	−0.065	0.068
	Be	0				0.228	0.037	1.001	0.351	0.274	0.015	0.100	−0.094	0.554
	Mg	0				0.243	0.067	0.597	0.359	0.286	0.006	0.052	−0.068	0.182
	Ca	0				0.231	0.047	0.832	0.356	0.280	0.020	0.061	−0.049	0.239
	Zn	0				0.250	0.078	0.493	0.361	0.289	0.006	0.085	−0.051	0.098
3	Li	0	0.224	0.027	1.434				0.354	0.269	0.017	0.033	−0.045	0.573
	Na	0	0.225	0.031	1.279				0.355	0.272	0.012	0.025	−0.033	0.234
	K	0	0.222	0.027	1.361				0.357	0.278	0.011	0.025	−0.024	0.137
	Cu	0	0.231	0.039	1.157				0.341	0.243	0.016	0.076	−0.055	0.211
	Be	2	0.232	0.029	1.576				0.341	0.241	0.013	0.075	−0.064	0.861
	Mg	2	0.234	0.041	1.178				0.348	0.255	0.013	0.042	−0.052	0.248
	Ca	2	0.225	0.026	1.464				0.355	0.273	0.009	0.044	−0.038	0.171
	Zn	2	0.245	0.058	0.925				0.342	0.238	0.015	0.069	−0.039	0.172

[a] ρ, *L*, and ϵ are the density, $-1/4\nabla^2\rho$, and the ellipticity at the (3,−1) critical points, respectively. All quantities are in atomic units.

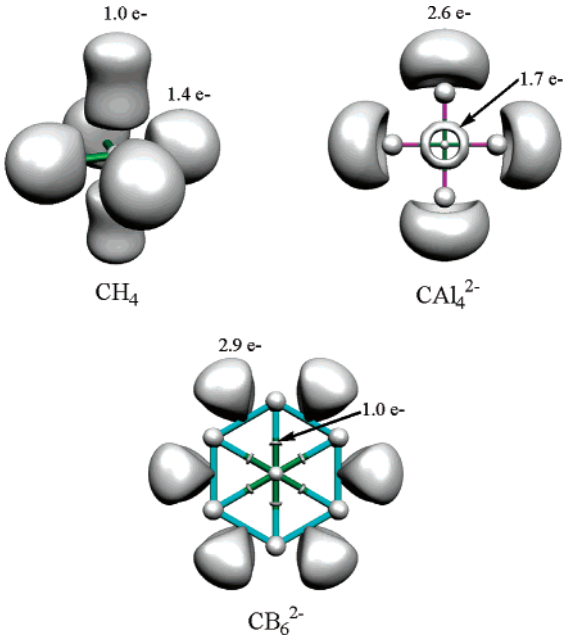

Figure 7. ELF isosurfaces (ELF = 0.8) for the planar CH_4, CAl_4^{2-}, and CB_6^{2-}. The numbers indicate the integration of the electron density in the corresponding basin.

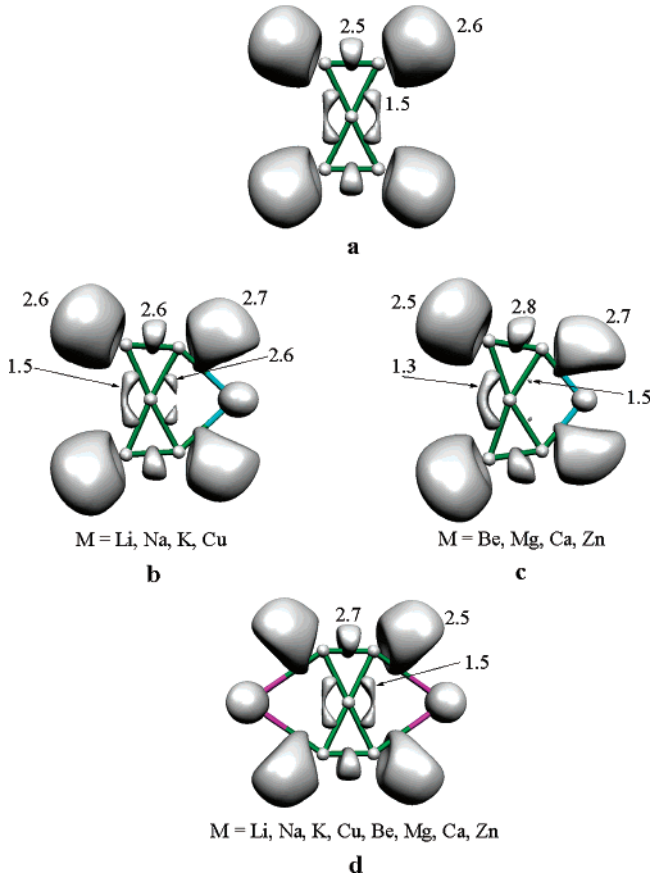

Figure 8. Isosurfaces of the ELF for (a) C_5^{2-}, (b) C_5M^-, (c) C_5M, and (d) $C_5M^{(0,2)}$, where M is the metal cation indicated at the bottom of the corresponding structure. The value of the isosurface is 0.8. The numbers indicate the integration of the electron density in the corresponding basin.

regarding the bonded and nonbonded electron pairs (Lewis model). One possibility to complement the nonempirical connectivity provided by the electron density is to use the electron localization function, ELF(**r**), proposed by Becke and Edgecombe.[39] This function is particularly suited to answer these questions because it displays separate basins corresponding to the core electrons and to the shared and unshared (lone pair) electron density of the valence shell. To gain familiarity with the shape of the ELF in ptC-containing molecules, Figure 7 depicts this molecular scalar field for planar CH_4, CAl_4^{2-}, and CB_6^{2-}. In planar methane, there are six basins around the carbon atom, four corresponding to C−H bonds and two basins, perpendicular to the molecular plane, related to the carbon lone pair. The populations of these basins are 1.4 and 1.0 e^-, respectively. In CAl_4^{2-} and CB_6^{2-}, there are four and six basins around the carbon atom integrating to 1.8 and 1.0 e^-, respectively. In these latter systems, the ELF does not have a maximum related to a lone pair. It is interesting to note that eventhough the carbon is surrounded by four (planar CH_4 and CAl_4^{2-}) or six (CB_6^{2-}) atoms, the population of the valence shell is only 6 e^-. Therefore, these systems are hypercoodinate molecules.

In C_5^{2-}, C_5M^-, and C_5M_2, there are four basins around the carbon atom, whose populations vary from 1.3 to 1.5 e^- (Figure 8). Similar to CAl_4^{2-} and CB_6^{2-}, the planar carbon atom does not have a lone pair perpendicular to the molecular plane. The

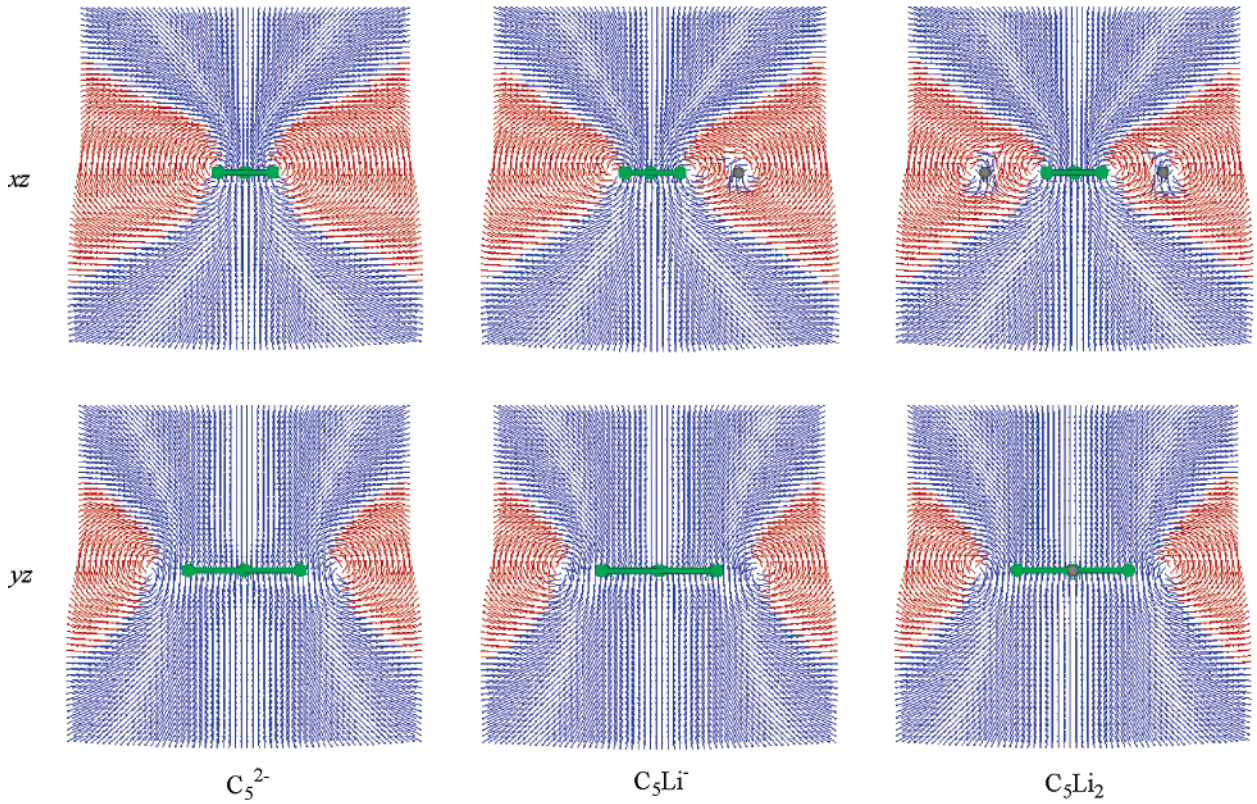

Figure 9. Induced magnetic field corresponding to an applied external field in the *z*-direction of C_5^{2-}, C_5Li^-, and C_2Li_2. The molecules are located at the *xy* plane, which is perpendicular to the planes depicted. Diatropic contributions are given in blue and paratropic contributions in red. In all cases, $B_{ext} = 1$ T.

external carbons have valence basins with populations between 2.5 and 2.7 e^-. This is attributed to a lone pair. In addition, the population of the valence basin associated with C_2 and C_2' changes from 2.6 to 2.9 e^-. From this point of view, the systems studied here are also hypercoordinate molecules. Since the metal basin is detached from the remaining part of the molecular system, one can conclude that the interaction between the metallic cation and C_5^{2-} is basically ionic.

Magnetic Properties. The magnetic properties have also been calculated for the $ptC(C)_4$ molecules. The NMR calculations reveal that the ^{13}C NMR chemical shifts are outside the typical ^{13}C shielding range of sp^2 carbons, which usually resonate between 120 and 220 ppm (Table 4). To gain a better understanding of this special behavior and to detect the presence of eventual cyclic electron delocalization, the nucleus-independent chemical shifts (NICS)[40] were calculated at the central position of the $C_2-C_1-C_2'$ triangle. All of the $ptC(C)_4$ molecules studied here have a strong diatropic NICS (Table 4), which denotes significant electron delocalization. An 11.6 ppm difference is observed between the largest and the smallest value. $C_5M_2^{0,2}$ molecules (M = alkaline or alkaline earth metal) are the most diatropic compounds, while the d^{10}-metal-containing systems show less diatropicity. Similarly, the $NICS_\pi$ index shows that the π-orbitals are strongly diatropic and contribute to the overall electron stabilization. The $NICS_\pi$ value of the C_5^{2-} indicates that this moiety has a larger π-diatropicity than that of the metal-containing molecules, as the cations localize the π electrons. In C_5^{2-}, $NICS_\pi$ is slightly larger than the total NICS, a situation that is reversed in the metal-containing systems. Therefore, an overall stabilization of the σ-system by the metal is involved. Besides, the paratropic character of the

Table 4. Magnetic Properties of **1**−**3**: NICS, HOMO−NICS, and ^{13}C Chemical Shifts (in parts per million)

	M	*n*	$^{13}C_1$	$^{13}C_2$	$^{13}C_2'$	$NICS_{tot}$	$NICS_\pi$	$NICS_{HOMO}$
1		2−	231.00	223.26		−30.2[a]	−37.9[a]	26.3[a]
2	Li	1−	230.77	220.10	207.18	−32.2	−29.1	19.3
	Na	1−	237.43	239.36	242.87	−31.7	−29.0	19.5
	K	1−	240.67	249.60	247.86	−31.7	−31.6	23.0
	Cu	1−	251.62	205.88	258.11	−27.9	−24.0	13.2
	Be	0	230.17	229.48	207.11	−33.6	−22.6	10.4
	Mg	0	242.28	263.42	267.80	−31.6	−22.3	11.0
	Ca	0	239.68	253.76	226.54	−33.5	−23.9	16.1
	Zn	0	256.18	269.57	319.06	−30.0	−19.7	8.2
3	Li	0	217.28	193.36		−34.7	−32.0	17.8
	Na	0	221.88	206.36		−34.6	−15.5	11.9
	K	0	226.26	211.49		−34.5	−17.2	14.9
	Cu	0	228.09	213.17		−28.6	−14.7	9.8
	Be	2	200.50	169.57		−39.5	−15.6	11.7
	Mg	2	207.67	189.70		−36.3	−20.0	9.4
	Ca	2	217.89	207.61		−36.3	−15.1	17.6
	Zn	2	210.87	219.91		−33.6	−22.3	7.4

[a] Calculated with PW91/IGLO-III.

σ-HOMO ($3b_{2u}$) is highly sensitive toward the nature and the number of cations. A factor of 3 is found when comparing the $NICS_{HOMO}$ values of the different molecules. Due to the Coulomb stabilization, the HOMO is less paratropic and consequently more stable when a second cation is added. In consequence, after a cation is added, the fraction of σ-diatropicity increases with the concomitant decrement of the π-contribution.

Additional information about the electronic delocalization is provided by the induced magnetic field ($\vec{B}_{ind}$) of a molecule when an external magnetic field perpendicular to the molecular plane is applied. Figure 9 shows the induced magnetic field of

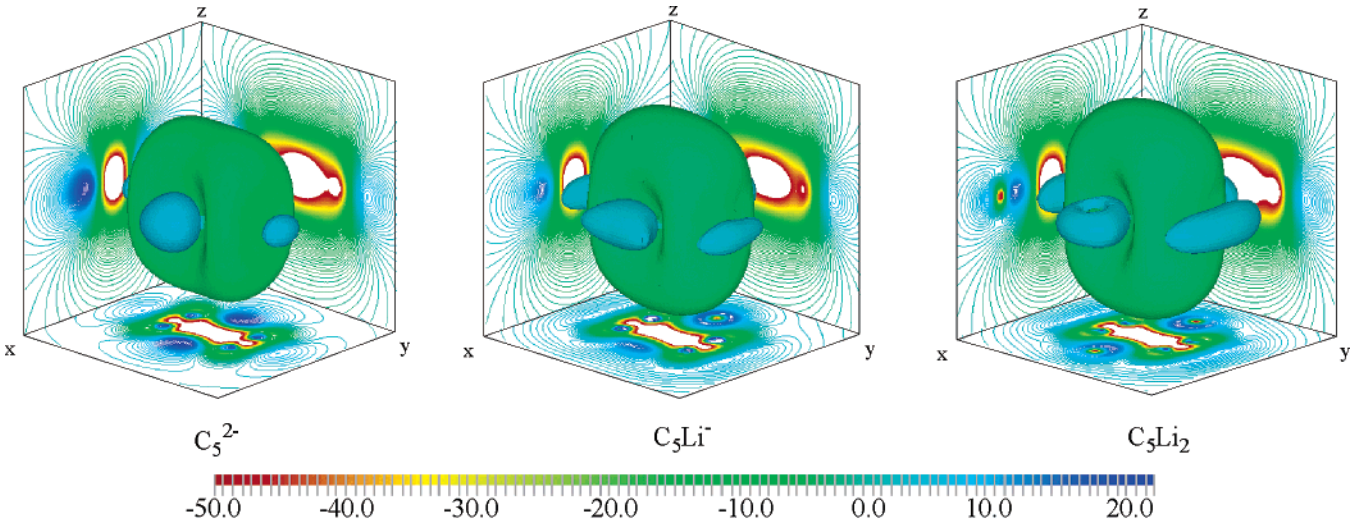

Figure 10. Isosurfaces and contour lines of the $(\vec{B}_{ind})_z$ of C_5^{2-}, C_5Li^-, and C_2Li_2. The value of the isosurface is 4 μT. Green and blue indicate shielding [$(B_{ind})_z < 0$] and deshielding regions, respectively. Contour lines of the $(\vec{B}_{ind})_z$ of planes passing through the molecular center are plotted at the faces of the box.

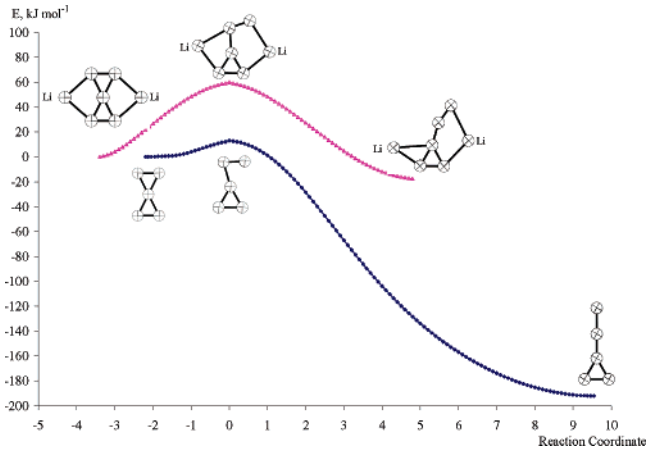

Figure 11. Energy profiles for the isomerization of C_5^{2-} and C_5Li_2. The points were obtained from IRC calculations. The origin of both reaction paths is the corresponding transition state.

C_5^{2-}, C_5Li^-, and C_5Li_2 located at the *xz* and *yz* planes and the isosurfaces of the *z*-component $(\vec{B}_{ind})_z$.[65] As it may be seen in these figures, strong diatropic contributions are observed inside the three-membered rings. This trend is a clear consequence of the π-delocalization and is similar to that of benzene and opposite to that of C_4H_4 (an antiaromatic system).[65] Around the σ-framework of C_5^{2-}, there are four nodal rings (one for each side of the rectangle), which separate shielding from deshielding regions. The addition of the lithium atoms generates new nodal rings around the lithium atom. The behavior is the same independently on the number of cations.

Figure 10 depicts the contour lines and the isosurface of the *z*-component of the induced magnetic field, $(\vec{B}_{ind})_z$, giving a quantification sight of the magnetic response. The isosurface of $(\vec{B}_{ind})_z$ shows that the shielding regions (in green) are located around the molecule, while deshielding regions are further outside (in blue). Again, this tendency is analogous to benzene and contrary to cyclobutadiene. It is also shown in Figure 10 that the response of the molecule to the magnetic field is long-ranged (see above and below the rings). In summary, the magnetic properties, NICS and $\vec{B}_{ind}$, show that the dianion and the salts have an important electron delocalization that contributes to enhance the stability of these chemical species.

Is it Possible To Detect a ptC(C)$_4$ Molecule? The ptC(C)$_4$ molecules reported herein are stabilized exclusively by electronic factors. The theoretical evidence presented and discussed in the previous sections indicates that C_5Li_2 is a good candidate for experimental isolation. This molecule has several interesting properties: it is planar, like the parent C_5^{2-} anion, it is the hardest, and it is one of the most diatropic compounds studied here. However, the experimental observation of C_5Li_2 would also depend on the possible rearrangements to more-stable isomers. For C_5^{2-}, the rearrangement barrier is only 12.6 kJ mol^{-1}, including the zero-point energy correction, but the inclusion of two lithium cations increases this barrier to 58.3 kJ mol^{-1} (Figure 11). Furthermore, the energy difference between the planar structure of C_5^{2-} and that of the closest isomer is -184.0 kJ mol^{-1}, while for C_5Li_2, this value is appreciably lower (-17.4 kJ mol^{-1}). Therefore, the isomerization barrier in C_5Li_2 is sufficiently high to support our optimism that this molecule can be experimentally detected.

Conclusions

An extensive search on the potential energy surface of C_5^{2-} reveals the existence of a local minimum with one planar tetracoordinate carbon for this anionic cluster. The addition of metallic cations to the parent C_5^{2-} structure generates species with the desired planar tetracoordinate carbon, which are stabilized exclusively by electronic factors. The optimized bond distances and the nonempirical connectivity provided by the topological analysis of the electron density support the tetracoordination of the central carbon atom. A comparative analysis of several molecular scalar fields, namely, the molecular orbitals, the electron density, and the electron localization function, indicates that the stability of the C_5^{2-} derivatives depend on the delocalization of the p-orbital. The nucleus-independent chemical shits and the induced magnetic fields of these chemical species also show that they have an important electron delocalization contributing to its stability. The overall analysis and the energy profile of the isomerization reaction indicate that

(65) Merino, G.; Heine, T.; Seifert, G. *Chem. Eur. J.* **2004**, *10*, 4367−4371.

the lithium salt, C_5Li_2, is the most plausible candidate for experimental detection.

Acknowledgment. This work was funded in part by grants from the Deutsche Forschungsgemeinschaft (DFG), Conacyt (Projects G34037-E and G32710-E), and the Swiss National Science Foundation (Grant 200020-100070).

JA047848Y